Available online at www.sciencedirect.com

ScienceDirect

www.elsevier.com/locate/jes

JES JOURNAL OF ENVIRONMENTAL SCIENCES

www.jesc.ac.cn

Development and validation of a thermally regulated atmospheric simulation chamber (THALAMOS): A versatile tool to simulate atmospheric processes

Noureddin Osseiran[1], *Manolis N. Romanias*[1,*], *Vincent Gaudion*[1], *Maria E. Angelaki*[2], *Vassileios C. Papadimitriou*[2,*], *Alexandre Tomas*[1], *Patrice Coddeville*[1], *Frederic Thevenet*[1]

[1] *IMT Lille Douai, Univ. Lille, SAGE, Lille F-59000, France*
[2] *Laboratory of photochemistry and chemical kinetics (LAPKIN), University of Crete, Heraklion 71003, Crete, Greece*

ARTICLE INFO

Article history:
Received 13 August 2019
Revised 24 January 2020
Accepted 17 March 2020
Available online 11 May 2020

Keywords:
Thermostated simulation chamber
Gas phase kinetics
Cl initiated degradation of toluene
Benzaldehyde

ABSTRACT

Atmospheric simulation chambers, are unique tools for investigating atmospheric processes in the gas and heterogeneous phases. They can provide a controlled yet realistic environment that simulates atmospheric conditions. In the current study, a Teflon atmospheric simulation chamber of 600 L, named THALAMOS (thermally regulated atmospheric simulation chamber) has been developed and cross-validated. THALAMOS can be operated over the temperature range 233 to 373 K under both static and flow conditions. It is equipped with state of the art instrumentation (selective ion flow tube mass spectrometry (SIFT-MS), long path Fourier transform infrared spectroscopy (FTIR), gas chromatography-mass spectrometry (GC-MS), various analyzers) for the in-line monitoring of both reactants and products. THALAMOS was validated by measuring the rate coefficients of well documented reactions, i.e. the reaction of ethanol with OH radicals and the reaction of dichloromethane with Cl atoms, in a wide temperature range. Two different detection techniques were used in parallel, FTIR and SIFT-MS, to internally cross-validate the obtained results. The measured rate coefficients are in excellent agreement, both between each other and with the literature recommended values. Furthermore, the gas phase oxidation of toluene by Cl atoms (kinetics and product yields) was studied in the temperature range of 253 to 333 K. To the best of our knowledge, THALAMOS is a unique facility on national level and among a few smog chambers internationally that can be operated in such a wide temperature range providing the scientific community with a versatile tool to simulate both outdoor and indoor physicochemical processes.

* Corresponding authors.
E-mails: emmanouil.romanias@imt-lille-douai.fr (M.N. Romanias), bpapadim@uoc.gr (V.C. Papadimitriou).

https://doi.org/10.1016/j.jes.2020.03.036
1001-0742/

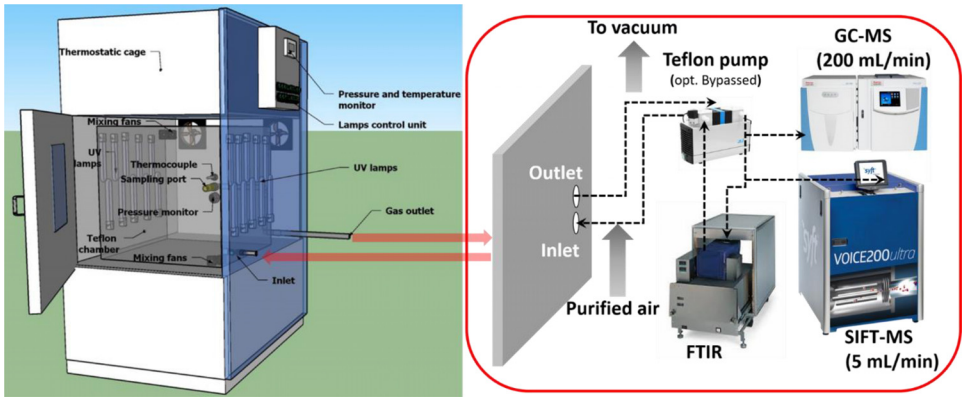

Fig. 1 – General description of THALAMOS (thermally regulated atmospheric simulation chamber) facility. UV: ultraviolet; FTIR: Fourier transformed infrared spectroscopy; GC-MS: gas chromatography mass spectrometry; SIFT-MS: selective ion flow tube mass spectrometry.

Introduction

Air pollution is one of the major concerns of our society nowadays. The intense anthropogenic activities related to combustion, industrialization, agriculture and livestock, release a wide variety of pollutants in the atmosphere affecting air quality. Furthermore, in the context of climate change and the anticipated global temperature change, as well as the increasing urbanization rate observed within the last 70 years (in 2015 around 80% of the population was living in urban areas in developed countries (United Nations, 2018)), the effects on air quality have been a top priority issue in the agenda of many countries. Therefore, a strong effort has been made by the atmospheric science community through multidisciplinary actions involving laboratory, field and modeling studies aiming to elucidate the important processes that lead to air pollution, to propose solutions and to make predictions regarding the future Earth's climate.

Hence, the thorough study of chemical processes occurring during night time or daytime in the atmosphere, is of great importance in order to (i) elucidate the fate of pollutants and investigate their impact to the physicochemical properties of the atmosphere, e.g., formation of organic aerosols and tropospheric O_3, stratospheric ozone depletion as well as to (ii) determine the lifetimes of pollutants and thus their impact on the future climate. However, the atmosphere is an open chemical reactor and thus the direct control or isolation of chemical processes is challenging. Alternatively, in laboratory scale, the investigation of key atmospheric phenomena can occur inside Atmospheric Simulation Chambers (ASC). ASC provide a controlled, yet realistic environment, aiming to simulating atmospheric conditions without any meteorological or emissive influences that occur in real atmosphere. Since the first ASC development (Akimoto et al., 1979; Leone et al., 1985) in the mid-1980s, several small to large-scale facilities have been developed worldwide aiming to study (i) gas phase reactions between the major atmospheric oxidants and both anthropogenic and biogenic volatile organic compounds (VOCs), (ii) secondary organic aerosol (SOA) formation and (iii) nucleation phenomena and/or processes related with air-quality and climate. In Europe, most of these facilities are integrated in the Eurochamp-2020 project and are accessible to the scientific community (Huang et al., 2012).

Generally, there are two types of simulation chambers: indoor and outdoor. They are also present in a wide range of volumes and forms, and can be constructed by several materials including Teflon, Pyrex glass, stainless steel etc.. However, till today, the majority of simulation chambers studies, especially the ones related to gas-phase chemistry, have been conducted close to ambient temperature and sea level pressure conditions. Atmospheric pressure and temperature though vary with the altitude. Particularly, temperature variation can strongly affect physicochemical phenomena (i.e. kinetics, reaction mechanism, nucleation processes, etc.) and plays a key role in several atmospheric studies.

Therefore, the objective of this study was to develop and validate an atmospheric simulation chamber, named THALAMOS (thermally regulated atmospheric simulation chamber), that can be used as a reference tool for temperature dependent studies simulating both outdoor and indoor environment. In this paper, we introduce THALAMOS to the scientific community presenting a detailed description of chambers' characteristics and capabilities. To the best of our knowledge, THALAMOS is the first ASC, on national level that allows temperature dependent studies, and one of very few facilities globally, with such a wide accessible temperature range, 233 – 373 K that fully covers relevant to the troposphere temperature range and can also be operated at higher temperatures, either to study extreme indoor conditions or to investigate reaction mechanism. Within this framework, a series of results that demonstrate both THALAMOS validity as a versatile tool for temperature dependent kinetics and end-products determination as well as the extent of its capabilities are presented herein. First, THALAMOS was validated by measuring the kinetics of the well documented gas phase reactions of OH radicals and Cl atoms with ethanol and dichloromethane (DCM), over a wide temperature range. Next, the Cl atoms rate coefficients for the gas phase reaction of Cl atoms with toluene were measured and the reaction mechanism was investigated, as a function of temperature. Finally, the obtained results are discussed. Toluene is an aromatic compound mainly emitted by anthropogenic activities and concentrations that can reach up to several hundreds of ppbV in outdoor (Hazrati et al., 2016) or working indoor environments (Can et al., 2015).

1. Materials and methods

1.1. *THALAMOS description and characteristics*

THALAMOS is an indoor, atmospheric simulation chamber with a volume of 0.6 m^3 (Fig. 1) that consists of three main parts, (i) a climatic thermostatic cage (VT-4100, Vötsch industrietechnik, Germany), (ii) a Teflon chamber of cuboid shape attached on an aluminum frame (see Fig. 1) and (iii) multiple in-line complementary detection techniques, such as Fourier transform infrared spectroscopy (FTIR), selective ion flow tube mass spectrometry (SIFT-MS), and gas chromatography-mass

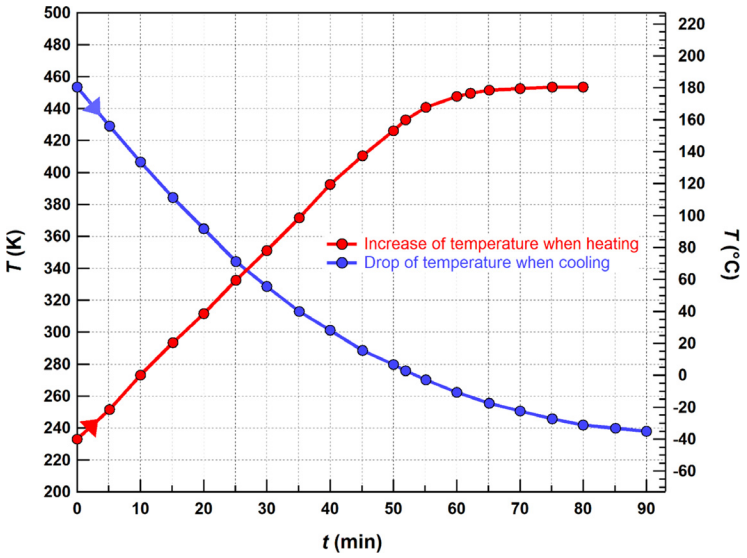

Fig. 2 – Temperature (T) dynamic in the climatic box determined under heating and cooling experiments. The arrows placed at the beginning of each curve aim to display the corresponding process followed to determine the temperature change rate. t: time.

spectrometry (GC-MS) that are assembled externally to the Teflon-chamber. The thermostatic cage (or climatic box) has an effective volume of 1200 L and the temperature can be regulated between 231 and 453 K. The climatic box is equipped with a platinum temperature sensor (PT-100, Pico technology, France) to measure the temperature and two fans to transfer and homogenize the heated/cooled air in the thermostatic cage (Fig. 1). Fig. 2 displays the temperature change rate inside the climatic box illustrating the facility efficiency to achieve extreme cold or hot conditions in a relatively short time window and to adequately simulate the relevant to the Troposphere conditions, in a very well controlled environment inside the Teflon-chamber.

The Teflon chamber volume was experimentally determined via absolute concentration measurement of ethylbenzene by employing Beer-Lambert low and using in-line infrared spectroscopy. Particularly, multiple titrated volumes of liquid ethyl-benzene ($C_6H_5CH_2CH_3$) were introduced via micro-syringe into the chamber, i.e., 0.1 – 0.5 mL, and the infrared (IR) spectra were recorded using 1 cm^{-1} resolution and 128 co-added scans. IR spectra were integrated between 2493 and 3492 cm^{-1}. Using an integrated band strength of 3.36×10^{-17} cm^2/(molecule·cm), and a density of 0.8626 g/cm^3 for ethyl-benzene, chamber volume was determined to be 601 ± 6 L (Lide, 2005). A temperature and pressure sensor were assorted in the center and back side of the Teflon chamber (see Fig. 1) and the gas mixture temperature/pressure were monitored in real-time. Both measurements were digitized and recorded and stored in a lab computer for further analysis.

The Teflon chamber is also equipped with four fans to ensure (i) the temperature homogeneity of the gas mixture and (ii) the efficient mixing of reagents. Particularly, the two fans are placed at the front and bottom-right side of the chamber, right after the inlet port and installed with a 45 degrees angle allowing the efficient transport of the injected compounds to the main body of the chamber. Two more fans are placed at the back and up-left side (Fig. 1). The temperature inside the thermostatic cage and the Teflon chamber were measured via two thermocouples and the readings comparison over a wide range are comparatively depicted in Appendix A Fig. S1. An excellent agreement - differences are lower than 1% in Kelvin scale, validating that the gas mixture in the Teflon chamber is effectively thermally-equilibrated throughout the reactor volume.

1.1.1. *Admission and mixing of compounds*

A multi-inlet port placed in the front and bottom-right side of the chamber was used for compounds introduction (Fig. 1). Depending on the physical state and volatility of compounds, different injection methods were applied.

(i) Injection of gas phase compounds.

Gases are introduced in the chamber either using gas syringes or via controlled flow through mass flow controllers.

(ii) Injection of liquid phase compounds.

For the injection of liquid phase compounds two different methods were applied. In the first method, liquid compounds were injected inside the chamber via a septum inlet using syringes, under a stream of zero-air. To facilitate the evaporation of the liquid, the introduction line was heated at 323 K by using heating taped inlets to control the temperature. Nevertheless, to ensure complete vaporization of the injected compounds, inlet-line's temperature can be increased up to 423 K, when needed, in the case of very low-volatile compounds. In the second method, gas mixtures of known concentrations were prepared in zero air and injected using mass flow controllers. In particular, compounds in the liquid phase were transferred to a glass tube that could be thermostated. Then using gas handling system equipped with Baratron pressure gauges, compounds' were either collected in 10 L glass-bulb or to a 6 L Silonite canister (both were previously evacuated to a pressure of 10^{-3} mbar) and further diluted to a total pressure of 1300 mbar for the glass-bulb and 2070 mbar for Silonite canister using zero-air as bath gas. The manometrically prepared mixtures were injected in the chamber using mass flow controllers under zero-air stream.

(iii) Reaction mixture homogenization.

Gas mixture homogenization inside THALAMOS, at 296 K, is achieved within ~1 min, but in general, it is also dependent on compound volatility, potent adsorption, hydrolysis or condensation onto chamber's surface and THALAMOS temperature. To ensure steady-state concentrations for all the species in the chamber, gas mixture was fan-mixed for, at least, 20 min before reaction's initiation, and the gas phase concentrations of the organic compounds were continuously monitored

to warrant steady-state using the analytical instrumentation described below.

1.1.2. Bath gas and Teflon chamber cleaning

In the majority of the THALAMOS runs, zero air is being used as bath gas, generated from an oil-free air-compressor, coupled with an in-line water removal system. Then, zero air could be further purified and provided to the chamber under a regulated constant flow. Depending on the purification process, two different zero air flows can be used. In the first case, the air produced is driven through a zero-air generator (AZ-2020, Claind, Italy) operated at 673 K to catalytically convert the organics present in the air flow to CO_2. The exact relative humidity (RH) in the gas flow at room temperature, 293 K, was determined to be 2% using a temperature and relative humidity probe (HQ 210, Kimo, France) with an accuracy ± 1% as stated by the manufacturer. Alternatively, the air-flow from the compressor is sent to a high purification system (zero-air generator equipped with a pressure swing adsorption (PSA) device), where volatile organic compounds (VOCs), CO_2, CO and H_2O are removed. The remaining impurity levels in the air stream are always lower than the analytical system detection limits: VOCs < 0.1 ppbV, CO_2 < 10 ppbV, CO < 80 ppbV and H_2O ~2 ppmV at 293 K. We estimate that NO_x and O_3 concentration levels in the chamber are below 50 and 500 pptV respectively (detection limits of NO_x analyzer (T200 UP, Teledyne, USA) and ozone analyzer (APOA 370, Horiba, France)). In addition, it is important to mention that when measurements in the presence of NO_x are carried out in THALAMOS, right after their completion, chamber's Teflon film , the tubing's and even the diaphragm in the Teflon pump are replaced to ensure that our system is clean and free of any memory effects in the future experiments.

Prior to each experiment, THALAMOS is flushed-out for at least 2 hours, using a constant flow of zero-air, i.e., 20 L/min and a similar pumped-out rate. The cleaning process is necessary in order to avoid any side reaction or accumulation of different reactants inside the chamber or dead-volumes, eliminating memory effects during sequential experiments.

1.1.3. Light sources and radicals/atoms precursors and production

In order to induce photo-oxidation reactions, the thermostatic cage has been equipped with a light irradiation system capable to host 20 lamps. More specifically, the attached broad-band emission light sources are (i) 10 ultraviolet (UV) lamps emitting in the UV-A region of electromagnetic spectrum, i.e. UV-A lamps (PL-L 24W/10/4P, Philips, Netherlands) with a maximum wavelength (λ_{max}) at 365 nm, and (ii) 10 mercury lamps (HNS-L 24W 2G11, Osram, UK) emitting UV radiation in the UV-C region of the electromagnetic spectrum, i.e. UV-C lamps, with a λ_{max} at 254 nm. Therefore, THALAMOS can be used to study any induced processes in the gas phase (e.g. photolysis of compounds of interest, or cross section measurements) or involving heterogeneous phase (e.g., TiO_2 photocatalysis). It should be noted that the heat released from the lamps (when switched on) does not impact the temperature inside THALAMOS. In particular, the response of the climatic box to temperature variations has been settled to a minimum of ±1 K, which is feasible due to the high performance of our heating/cooling system. Gas mixture temperature inside THALAMOS is maintained stable (±1 K) and any variations are continuously monitored, both inside and outside the Teflon chamber, during the course of all the photochemical experiments.

In the current study, UV-A lamps were used to generate Cl atoms via Cl_2 photolysis:

$$Cl_2 + h\nu \rightarrow 2\,^{\bullet}Cl \quad (1)$$

Similarly, the UV-C lamps were used to photolyze H_2O_2 and produce OH radicals via the reaction:

$$H_2O_2 + h\nu \rightarrow 2\,^{\bullet}OH \quad (2)$$

where $h\nu$ corresponds to the light source photon-energy. Please note that in the whole article, OH and Cl notation refer to radicals and atoms, respectively, and electron symbol is omitted for simplicity.

1.1.4. Reaction mixture sampling and detection techniques

A Restek Sulfinert-treated stainless steel tube was placed in the center and back-side of the chamber, allowing the reaction mixture sampling-off the chamber. Stable reactants and products were continuously monitored via in-series coupling of the chamber with several detection methods and sensors, with the main ones to be (i) a SIFT-MS (Voice 200 ultra, Syft Technologies, New Zealand), (ii) a multipath FTIR (Antaris IGS, Thermo Scientific, France) with an optical path of 10 m and (iii) a thermal desorption GC-MS (7890A, Agilent Technologies, France). The complementary detection techniques provides with the advantage to identify a great variety of chemical species with high sensitivity. Further, they provide a cross-validation measure and allow to minimize intrinsic uncertainties in temporal loss and formation profiles measurements for reactants and products, respectively. Sample-out rate was adjusted in a case by case experiment, according to the analytical methods employed at each measurement. Particularly, a recycling Teflon diaphragm pump, 4 L/min, is used to create a closed-loop between the chamber and the analytical instruments. In the case that solely SIFT-MS is used, reaction mixture was continuously sampled-out with a flow rate of 5 to 25 mL/min. Given that experiments duration was less than two hours, a negligible gas-mixture volume was lost <0.5%, taking into account experimental uncertainties. FTIR optical cell is part of the closed-loop and thus does not alter the gas volume. Finally, although it was not used in the present study, it is worth to note that GC-MS could be also used simultaneously in THALAMOS, since the amount of the required reaction mixture for the analysis is insignificant (~200 mL/min), compared to THALAMOS volume. It is also worth mentioning that in all cases results were cross-validated using simultaneously at least two independent detection methods, and the required sampling did not result in any measurable alteration of reactants concentrations, within the precision of the measurements.

The SIFT-MS is a tandem chemical ionization mass spectrometer based on the chemical ionization of the analytes. A microwave discharge is used for the simultaneous generation of three precursor ions, H_3O^+, NO^+ and O_2^+, which are sequentially selected by a first quadrupole mass filter (Smith and Spanel, 2005; Spanel and Smith, 2013). Then, the precursor ions are injected inside a flow tube reactor operated at mTorr pressure using N_2, as carrier gas. At the same time, the sample is injected at the upstream-end of the reactor. The precursor ions react with the analytes along the flow tube to produce new characteristic ionized molecules (Smith and Spanel, 2005; Spanel and Smith, 2013). It is worth mentioning that both the sampling port and the flow tube of the instrument are heated to 393 K to eliminate contaminations of the sampling line and wall reactions along the flow tube. Subsequently, the gas flow passes through a pinhole orifice of 0.3 mm diameter, located at the downstream end of the flow tube reactor to create a molecular beam. The molecular beam enters a differentially-pumped high vacuum chamber and both the precursor and reaction product-ions are focused, via electrostatic lenses, into a second quadrupole mass spectrometer for mass analysis and ion counting for identification and quantification, respectively. The mass spectrometer is internally calibrated on a daily basis, by flowing a standard mixture of 9 compounds provided by the supplier. The internal calibration procedure and the known reaction rate coefficients of the precursor ions with the analytes, allow estimating the theoretical concentrations of any organic compound. Nevertheless, to obtain accurate concentration measurements, the in-

strument was regularly calibrated by passing standards of the compounds of interest. Although in kinetic measurements the absolute concentrations are not used, it is worth mentioning that the difference between estimated theoretical concentrations and the ones determined experimentally were in fairly reasonable agreement with the observed differences never being higher than 30%. Instrument's time resolution depends on the number of mass spectral peaks monitored, as well as on the number of the averaging counts. For instance, the real time monitoring of 20 mass spectral intensities with a limit of 10,000 counts for each mass, time resolution was ca. 10 sec. Under these conditions, the detection limits for ethanol, dichloromethane and toluene were 1.0, 0.8 and 0.9 ppbV, respectively.

Complementary to the SIFT-MS, the reaction mixture was simultaneously analyzed employing an FTIR spectrophotometer equipped with a 10 m path length White-cell, with anti-reflected coated zinc selenide transmission windows. A liquid-N_2 cooled mercury cadmium telluride (MCT) detector was attached and 64 co-added IR spectra were recorded between 650 and 4000 cm^{-1}, with 1 cm^{-1} resolution, using Result-3 software. Quantification and data processing was performed using a thermos scientific software, TQ-Analyst™, and internally developed routines for kinetic analysis. The optical path was also experimentally calibrated using compounds with well-known IR cross-sections and it was determined to be 10.0 ± 0.1 m that is in excellent agreement with manufacturer technical data. The detection limits for ethanol, dichloromethane and toluene were in the ppmV range (~1 ppmV).

Background IR spectra were collected before compounds injection in the chamber. Note that a Teflon circulating pump was used in a closed loop to ensure gas-phase mixture homogeneity between chamber and FT-IR cell. After recording the background, reaction mixture was introduced in the chamber and left until it was well-mixed. Well-mixing was verified by recording sequential IR spectra. The steady-state concentrations of the reactants in the Teflon chamber was achieved after a few minutes and was verified by observing characteristic peaks stability using FTIR. Note that characteristic IR absorption bands reached a steady absorbance (±1%) within a few minutes and reactants stability was also cross-checked by monitoring the compounds concentration profiles using SIFT-MS.

1.1.5. *THALAMOS first-order losses*

n-Pentane (C_5H_{12}) was used as probe molecule aiming to evaluate possible leaks of THALAMOS. In this series of experiments, 30 ppmV of *n*-pentane was injected in the chamber and its temporal profile was monitored for several hours using the SIFT-MS. A typical plot, 293 K, is shown in Appendix A Fig. S2. The first order loss of pentane was measured to be ~10^{-6} sec^{-1} and it is not expected to affect the kinetic measurements, within the duration time of the actual kinetic measurements. Similar tests were carried-out between 253 and 353 K leading to identical results. However, since wall-loss and on-surface hydrolysis is also an intrinsic variable of the compound used (volatility, functionality, chemical affinity, etc.), dark-loss tests were carried-out in a case-by-case basis, before every experimental series runs.

1.2. *Relative rate measurements*

In this section, THALAMOS validation approach is presented. Two well-studied gas phase reactions, i.e., OH radicals with ethanol (C_2H_5OH) and Cl atoms with dichloromethane (DCM, CH_2Cl_2), were studied between 253 and 363 K at 760 Torr, in the presence of zero air. Further, kinetics and end-oxidation products for the reaction of Cl atoms with toluene (C_7H_8) were also determined. In all cases, the kinetic measurements were performed applying the relative rate method (RR).

In RR method the temporal loss of the under study compound (M) is measured relative to that of a reference compound (REF) ensuring that the observed changes are solely due to their reaction with the oxidant of interest X (X: OH, Cl, NO_3, O_3). RR method is a widely used method (Atkinson et al., 2006; Burkholder et al., 2015) and the relative rate coefficient is derived by the expression (King, 2016):

$$\ln\left(\frac{[M]_0}{[M]_t}\right) = \frac{k_M}{k_{REF}} \ln\left(\frac{[REF]_0}{[REF]_t}\right) \quad (3)$$

where $[M]_0$, $[REF]_0$, $[M]_t$, and $[REF]_t$ are the initial concentrations of the compound of interest and that of the reference, at reaction time $t = 0$, and at discrete times (t) after reaction mixture irradiation and k_M and k_{REF} are the corresponding second order rate coefficients, respectively. A relative rate plot, $\ln([M]_0/[M]_t)$ versus $\ln([REF]_0/[REF]_t)$, should be linear, with a slope equal to rate coefficients ratio, k_M/k_{REF}, and a zero intercept. Therefore, the rate coefficient for the reaction of interest can be determined from the relative rate data fitting relative to the known rate coefficient of the reference reaction (k_{REF}) (King, 2016).

Dark loss and photolysis tests were always conducted before rate coefficient measurements to ensure that both reactants are only lost via the reaction with the reactive species, while reactants well-mixing was verified before irradiation. In all measurements presented herein, UV-A and UV-C lamps photolysis loss was negligible for all the compounds the study involves, within the time frame of the experiment, while no measurable dark-loss were observed.

1.3. *Experimental protocol*

Prior to each relative rate experiment, the chamber was continuously flushed with zero-air (cleaning process). Next, the background concentrations of the compounds of interest were measured using all the employed detection techniques. In kinetics determinations and at temperatures above 293 K, reactants and radical precursors were introduced in the chamber, once the desired chamber temperature had been reached. At lower temperatures than 293 K, the reaction mixture was introduced at room temperature and then the desired temperature was set. Reactants concentration was monitored through the whole time until the final temperature adjustment of the chamber to monitor any potent wall loss processes. Two criteria are required to be fulfilled before initiating the reaction: (i) the temperature in the climatic box to be equal to ±1 K with that of the gas mixture recorded inside the Teflon chamber, and (ii) the concentration profiles of organic compounds to be stable. Then, the reaction is initiated by switching on the UV-A or UV-C lamps, which photolyzes the OH radicals or Cl atoms precursors, respectively. Reactants consumption and products formation is then continuously recorded, as a function of time.

1.4. *Materials*

All chemicals used in the current study are commercially available and listed in Appendix A Table S1 along with their stated purities. The mass spectrometric ion peaks selected to monitor the concentration profiles of reference and target molecules are listed in Table 1.

2. Results and discussion

2.1. *THALAMOS validation for kinetic measurements*

In this section, OH radicals and Cl atoms kinetics for their reaction with ethanol and DCM, respectively, are presented.

Table 1 – Mass spectral ions intensities selected to monitor the concentration profiles of the compounds used in the current study.

Compound	Product ions used monitored	Mass to charge ratio (*m/z*)	Precursor ion
Ethanol	$C_2H_5O^+$	45	NO^+
n-Pentane	$C_3H_6^+$	42	O_2^+
Dichloromethane (DCM)	$CH(^{35}Cl)\ (^{35}Cl)^+$	83	NO^+
Acetone	$C_3H_6O^+$	58	O_2^+
2,2,2-Trifluoroethanol	$[CF_3CH_2OH]H^+$	101	H_3O^+
Methane	$CH_3O_2^+$	47	O_2^+
Toluene	$C_7H_8H^+$	93	H_3O^+
	$C_7H_8^+$	92	NO^+
	$C_7H_8^+$	92	O_2^+
Ethane	$C_2H_4^+$	28	O_2^+
Methanol	CH_5O^+	33	H_3O^+
	NO^+CH_3OH	62	NO^+
	CH_3O^+	31	O_2^+
Butanone	$C_4H_9O^+$	73	H_3O^+
	$NO^+C_4H_8O$	102	NO^+
	$C_4H_8O^+$	72	O_2^+
Benzaldehyde	$C_7H_7O^+$	107	H_3O^+
	$C_7H_5O^+$	105	NO^+
	$C_7H_5O^+$	105	O_2^+
Benzyl alcohol	$C_7H_7^+$	91	H_3O^+
	$C_7H_8O^+$	108	NO^+
	$C_7H_8O^+$	108	O_2^+
Benzyl hydroperoxide	$C_7H_8O_2^+$	124	H_3O^+
	$NO^+\ C_7H_8O_2^+$	154	NO^+

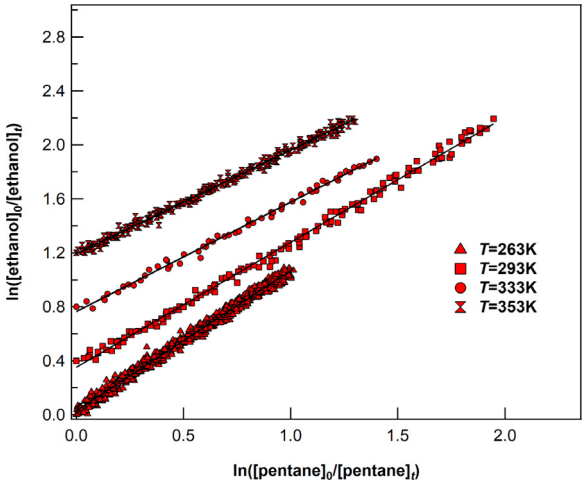

Fig. 3 – Relative rate data for the reaction of OH + ethanol using pentane as reference molecule at 263, 293, 333 and 353 K respectively. For clarity, the experimental measurements are shifted up on the y axis by 0.4 for 293 K, 0.8 for 333 K and 1.2 for 353 K. $[ethanol]_0$, $[pentane]_0$, [ethanol]t, $[pentane]_t$ are the initial concentrations of the compound of interest (ethanol) and that of the reference (pentane), with no OH radicals present (light-sources off), at t = 0 and at discrete reaction times t, respectively.

There were multiple reasons for choosing the abovementioned reactions. First, both reactions are of atmospheric interest; in particular, the study of atmospheric relevant reactions initiated by OH radicals (the major tropospheric oxidant) and Cl atoms (important tropospheric oxidant in coastal and urban areas) is of significant importance in order to determine the fate of pollutants in the atmosphere and thus their impact on air-quality and climate change. Secondly, the rate coefficients of both reactions have been extensively studied and the kinetic data have been evaluated by both International Union of Pure and Applied Chemistry (IUPAC) and the National Aeronautics and Space Administration/Jet Propulsion Laboratory (NASA/JPL) Panels. Therefore, these reactions were selected to evaluate THALAMOS reliability to measure relative rate coefficients over a wide temperature range, 253 – 353 K and thus its capability to provide accurate kinetic data of atmospheric relevant reactions.

2.1.1. *OH radical reaction rate coefficients with ethanol*

The gas phase reaction of OH radicals with ethanol has been a subject of interest for more than 3 decades (Campbell et al., 1976; Dillon et al., 2005; Greenhill and Ogrady, 1986; Jiménez et al., 2003; Kovács et al., 2005; Nelson et al., 1990; Oh and Andino, 2001; Orkin et al., 2011; Overend and Paraskevopoulos, 1978; Picquet et al., 1998; Ravishankara and Davis, 1978; Sørensen et al., 2002; Wallington and Kurylo, 1987; Wayne and Tully, 1988; Wu et al., 2003). For the determination of the bimolecular rate coefficient, both absolute and relative rate methods have been employed. Early published data were in large disagreement between each other (Campbell et al., 1976; Greenhill and Ogrady, 1986; Overend and Paraskevopoulos, 1978; Wallington and Kurylo, 1987; Wayne and Tully, 1988) with the problem to become even more intense between the temperature dependent kinetic studies (Greenhill and Ogrady, 1986; Wallington and Kurylo, 1987; Wayne and Tully, 1988). Nevertheless, the latest temperature dependent studies by Jimenez et al. (2003), Dillon et al. (2005) and Orkin et al. (2011) are in excellent agreement. It is worth mentioning that, to the best of our knowledge, all the temperature dependent studies have been carried out using absolute rate methods and thus the present work is the first temperature dependent study using relative rate methods. Literature data have been reviewed by both NASA/JPL and IUPAC kinetics panels (Atkinson et al., 2006; Burkholder et al., 2015). In particular, IUPAC panel has adopted two different expression depending on the temperature region of interest: $k(210-300\ K) = 3.2 \times 10^{-12} \exp(\frac{20}{T})$ cm^3/(molecule·sec) and $k(216-599\ K) = 6.7 \times 10^{-18} T^2 \exp(\frac{511}{T})$ cm^3/(molecule·sec) (Atkinson et al., 2006). On the other hand, NASA/JPL panel preferred values are based on the comprehensive absolute rate coefficient measurements at sub-ambient temperatures by Jiménez et al. (2003), Dillon et al. (2005) and Orkin et al (2011). Therefore, a temperature independent reaction rate coefficient ($k(210-298\ K) = 3.35 \times 10^{-12}$ cm^3/(molecule·sec) (Burkholder et al., 2015)) is recommended between 210 and 298 K.

In the current study, the kinetics of OH reaction with ethanol were studied in THALAMOS within the temperature range of 263 to 353 K, using OH + *n*-pentane as reference reaction. The SIFT-MS was employed for the real time monitoring of ethanol and the reference compound using the mass peaks 45 ($C_2H_5O^+$) and 42 ($C_3H_6^+$) employing NO^+ and O_2^+ precursor ions chemistry, respectively (see also Table 1). The temperature dependent rate coefficients for the reference reaction have been adopted from the recent review study from Morin et al. (2015) and was $k_{(OH+n-pentane)} = 9.0 \times 10^{-17} \times T^{1.8} \exp(\frac{120}{T})$ cm^3/(molecule·sec). The initial concentrations of ethanol and reference compound were between 3 – 4.5 ppmV, while H_2O_2 was ranged between 90 – 500 ppmV. The summary of the experimental conditions and the rate coefficients values obtained are given in Table 2. Typical relative rate kinetic profiles are shown in Fig. 3, the NO^+ and O_2^+ precursor ions were selected to monitor the concentrations of ethanol and pentane, respectively. Solids lines are the linear least-squares fits of the data and the fit results are given in Table 2. The rate coefficient values determined in the current study, along with the recommended literature values from IUPAC and NASA/JPL

Table 2 – Experimental conditions and kinetics results for the gas phase reaction of OH radicals with ethanol and Cl atoms with DCM.

$C_2H_5OH + OH$

T (K)	$[Ethanol]_0$ (ppmV)	$[Pentane]_0$ (ppmV)	$[H_2O_2]_0$ (ppmV)	$k_{ethanol}/k_{pentane}$ [a]	k ($\times 10^{-12}$ cm^3/(molecule•sec))[b]
263	3.1	3.0	300	1.04±0.01	3.35±0.03
278	3.2	3.0	90	0.97±0.01	3.37±0.03
293	3.5	3.4	250	0.93±0.01	3.40±0.04
	3.4	3.5	380	0.91±0.01	
	3.6	3.6	95	0.89±0.01	
313	3.7	3.7	90	0.85±0.01	3.48±0.04
333	4.0	3.9	450	0.81±0.01	3.63±0.04
353	4.2	4.1	500	0.77±0.01	3.75±0.05

$CH_2Cl_2 + Cl$

Reference: methane, $k_{(methane + Cl)} = 7.1 \times 10^{-12} \exp(-1270/T)$ cm^3/(molecule·sec), JPL recommended over 181-1550 K

T (K)	$[DCM]_0$ (ppmV)	$[Methane]_0$ (ppmV)	$[Cl_2]_0$ (ppmV)	$k_{DCM}/k_{methane}$ [a]	k ($\times 10^{-13}$ cm^3/(molecule•sec))[b]
258	2.8	21	80	4.16±0.05	2.15±0.03
270	2.9	16.6	61	3.81±0.02	2.45±0.02
298	3.8	18.1	36	3.48±0.02	3.49±0.02
	3.2	20.8	40	3.50±0.02	
323	3.4	20	48	3.16±0.02	4.36±0.03

Reference: acetone, $k_{(acetone + Cl)} = 1.63 \times 10^{-11} \exp(-610/T)$ cm^3/(molecule·sec), JPL recommended over 210-440 K

T (K)	$[DCM]_0$ (ppmV)	$[Acetone]_0$ (ppmV)	$[Cl_2]_0$ (ppmV)	$k_{DCM}/k_{acetone}$ [a]	k ($\times 10^{-13}$ cm^3/(molecule·sec))[b]
253	2.7	1.0	56	0.15±0.01	2.22±0.14
273	2.9	1.0	34	0.16±0.01	2.72±0.17
298	3.2	1.1	6.3	0.18±0.01	3.79±0.21
298	1.9	0.6	7.4	0.17±0.01	3.57±0.21
323	3.4	1.2	8.0	0.19±0.01	4.68±0.24
353	2.28	0.7	17	0.19±0.01	6.08±0.28

Reference: 2,2,2-trifluoroethanol, $k_{(trifluoroethanol + Cl)} = (6.85 \pm 0.8) \times 10^{-13}$ cm^3/(molecule·sec) at 298 K

T (K)	$[DCM]_0$ (ppmV)	$[Trifluoroethanol]_0$ (ppmV)	$[Cl_2]_0$ (ppmV)	$k_{DCM}/k_{trifluoroethanol}$ [a]	k (10^{-13})[b]
298	2.1	1.1	6.0	0.52±0.01	3.56±0.07
298	1.1	0.7	5.0	0.51±0.01	3.49±0.07
298 (FTIR)	15	15	88	0.49±0.02	3.35±0.14

$[M]_0$: initial concentration of the compound M; T: temperature; $k_{ethanol}$ / $k_{pentane}$: the experimentally determined relative rate coefficient ratios of the ethanol and the reference compound; k_{DCM} / $k_{methane}$, k_{DCM} / $k_{acetone}$, and k_{DCM} / $k_{trifluoroethanol}$: the experimentally determined relative rate coefficient ratios of DCM and the three reference compounds used (i.e. methane, acetone, trifluoroethanol), respectively; $k_{(methane + Cl)}$, $k_{(acetone + Cl)}$, and $k_{(trifluoroethanol + Cl)}$: the rate coefficients of methane, acetone and trifluoroethanol with Cl atoms as proposed in literature; k: is the final value of the rate coefficient of the compound of interest; NASA/JPL: National Aeronautics and Space Administration/Jet Propulsion Laboratory.

[a] Errors represent the 2σ precision from the least-squares fits and do not include systematic uncertainties.

[b] Errors reflects the 2σ precision of the relative rate ratio measurements and do not include any systematic uncertainty.

are depicted in Fig. 4. One can notice an excellent agreement between the measured rate coefficients and the IUPAC and NASA/JPL recommended values (±3%) within the entire temperature range experiments performed. Therefore, it is evidenced that THAMALOS is capable of determining the rate coefficient of OH initiated reactions as a function of temperature.

2.1.2. *Cl atoms reaction rate coefficients with DCM*

The rate coefficient for the reaction of Cl atoms with DCM has been widely studied and kinetic data are very well-established (Beichert et al., 1995; Bryukov et al., 2003; Catoire et al., 1996; Clyne and Walker, 1973; Davis et al., 1970; Niki et al., 1980; Orlando, 1999; Sarzyński et al., 2011; Tschuikow-Roux et al., 1988). Both absolute and relative rate measurements have been carried out to determine the temperature dependent rate coefficient (see Fig. 5). The reported data have been reviewed by IUPAC and NASA/JPL kinetics evaluation panels and the recommended expressions are $k\ (220 - 300\ K) = 5.9 \times 10^{-12} \exp(-\frac{850}{T})$ cm^3/(molecule·sec) (IUPAC) and $k\ (273 - 790\ K) = 7.4 \times 10^{-12} \exp(-\frac{910}{T})$ cm^3/(molecule·sec) (NASA/JPL).

In the current study, the rate coefficient for the gas phase reaction of Cl atoms with DCM was measured as a function of temperature using two reference compounds, i.e., methane (CH_4) ($k_{(methane + Cl)} = 7.1 \times 10^{-12} \exp(-1270/T)$ cm^3/(molecule·sec), NASA/JPL recommended over 181-1550 K) and acetone ($CH_3C(O)CH_3$) ($k_{(acetone + Cl)} = 1.63 \times 10^{-11} \exp(-\frac{610}{T})$ cm^3/(molecule·sec), recommended by NASA/JPL panel (Burkholder et al., 2015)). Furthermore, a series of experiments were carried out at room temperature using 2,2,2-trifluoroethanol (CF_3CH_2OH) as reference, an average value of $k_{(trifluoroethanol + Cl)} = (6.85 \pm$

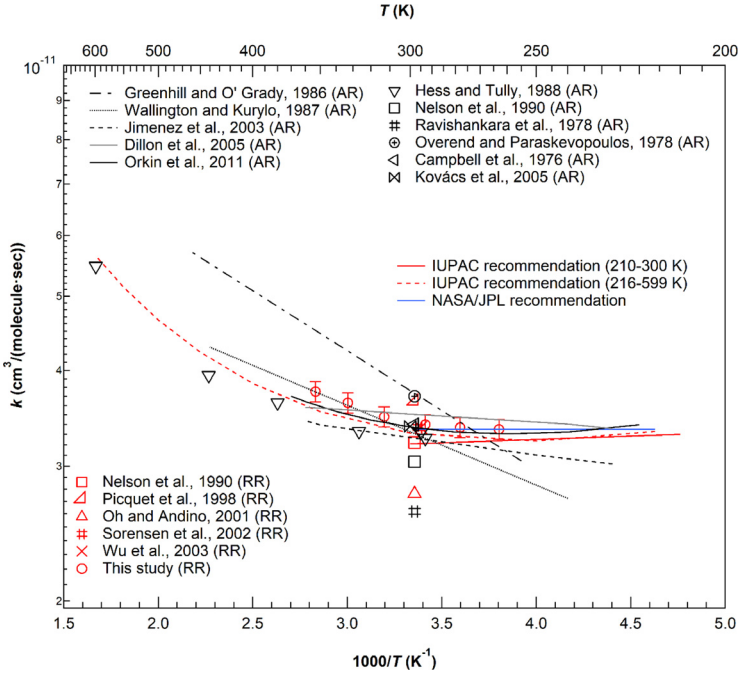

Fig. 4 – Arrhenius plot for the OH + ethanol reaction. In comparison with the measurements of the current study, are displayed the literature results determined with absolute methods (AR) and relative rate methods (RR) as well as the International Union of Pure and Applied Chemistry (IUPAC) and the National Aeronautics and Space Administration/Jet Propulsion Laboratory (NASA/JPL) recommended values. For clarity purposes, the uncertainties on literature results are not given; only the 2σ precision of the measurements (<2%) of the current study are displayed.

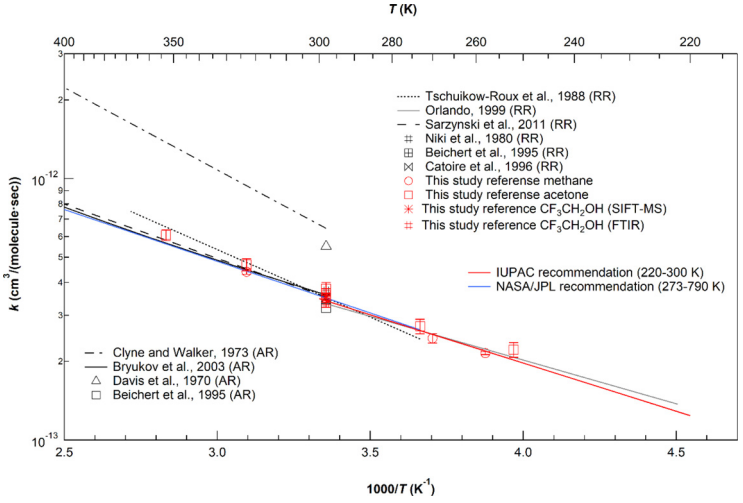

Fig. 5 – Arrhenius plot for the reaction of Cl atoms with DCM. For clarity purposes the NASA/JPL recommended values above 400 K are not displayed.

0.8) × 10^{-13} cm^3/(molecule·sec) was calculated from literature studies at 298 K (Garzón et al., 2010; Papadimitriou et al., 2003; Sellevåg et al., 2004) to cross validate the rate coefficients measured using SIFT-MS and FTIR as detection techniques. The SIFT-MS mass peaks used to monitor the reactants are summarized Table 1. FTIR kinetics analysis was carried out employing the subtraction method in which the recorded spectra during reactions progress were subtracted from scaled to the initial compounds concentration reference spectra recorded, separately, for each compound. In all the cases, multiple bands for DCM and $CH_3C(O)CH_3$ or CF_3CH_2OH were monitored and it was ensured that the selected peaks were zeroed. Products contribution was either subtracted, where possible, or taken into account, in cases where interference was intense and hard to resolve. Experiments at which differential IR spectroscopy was employed were also carried out. In that case, products appeared as positive peaks, while reactants as negative. Differential analysis also led to indiscernible results. The experimental conditions and the rate coefficient values determined are given in Table 2. Typical relative rate profiles are presented in Appendix A Fig. S3 and rate coefficients are summarized in the Arrhenius plot (Fig. 5). Kinetic results from the present study are in excellent agreement with the corresponding recommended literature

Table 3 – Summary of the experimental conditions and rate coefficients obtained in this work for the gas phase reaction of toluene with Cl atoms.

Reference: Ethane. $k_{(ethane + Cl)} = 7.05 \times 10^{-11}$ exp(-60/T), IUPAC recommended over 180-330 K

T (K)	$[Toluene]_0$ (ppmV)	$[Ethane]_0$ (ppmV)	$[Cl_2]_0$ (ppmV)	$k^{H_3O^+}_{toluene}/k^{O_2^+}_{ethane}$ [a]	$k^{NO^+}_{toluene}/k^{O_2^+}_{ethane}$ [a]	$k^{O_2^+}_{toluene}/k^{O_2^+}_{ethane}$ [a]	Variation [b]	$k_{toluene}/k_{ethane}$ of all ions [c]	k ($\times 10^{-11}$ cm^3/(molecule·sec)) [c]
253	3.3	3.3	22	1.14±0.08	1.16±0.08	1.19±0.04	4%	1.16±0.03	6.45±0.17
273	3.6	3.6	20	1.00±0.01	1.00±0.01	0.98±0.01	2%	0.99±0.01	5.60±0.06
293	3.8	3.8	15	1.02±0.02	1.01±0.01	1.03±0.01	2%	1.02±0.01	5.86±0.06
293	5.6	5.6	15	1.03±0.02	1.01±0.01	1.02±0.01	2%	1.02±0.01	
313	4.1	4.1	11	0.98±0.02	1.00±0.02	1.02±0.01	4%	1.00±0.02	5.82±0.12
333	4.3	4.3	17	0.99±0.04	1.00±0.04	0.99±0.02	1%	1.00±0.01	5.89±0.06

Reference: Methanol. $k_{(methanol + Cl)} = 7.10 \times 10^{-11}$ exp(-75/T), IUPAC recommended over 200-500 K

T (K)	$[Toluene]_0$ (ppmV)	$[Methanol]_0$ (ppmV)	$[Cl_2]_0$ (ppmV)	$k^{H_3O^+}_{toluene}/k^{H_3O^+}_{methanol}$ [a]	$k^{NO^+}_{toluene}/k^{NO^+}_{methanol}$ [a]	$k^{O_2^+}_{toluene}/k^{O_2^+}_{methanol}$ [a]	Variation	$k_{toluene}/k_{methanol}$ of all ions [c]	k ($\times 10^{-11}$ cm^3/(molecule·sec)) [c]
253	3.4	3.4	33	1.02±0.01	0.97±0.01	1.08±0.02	10%	1.02±0.06	5.38±0.32
268	3.3	4.1	17	1.20±0.01	1.07±0.02	1.18±0.01	11%	1.15±0.07	6.17±0.38
278	1.7	1.8	10	1.11±0.01	0.97±0.02	1.12±0.01	13%	1.07±0.08	5.80±0.43
278	3.5	4.5	20	1.06±0.01	1.04±0.02	1.10±0.01	5%	1.07±0.03	
293	1.9	2.0	11	1.08±0.01	0.96±0.02	1.07±0.01	11%	1.04±0.07	5.72±0.38
333	2.1	2.2	12	0.99±0.01	0.95±0.02	1.05±0.01	10%	1.00±0.05	5.68±0.28

Reference: Butanone. $k_{(butanone + Cl)} = 3.05 \times 10^{-11}$ exp(80/T), IUPAC recommended over 200-450 K

T (K)	$[Toluene]_0$ (ppmV)	$[Butanone]_0$ (ppmV)	$[Cl_2]_0$ (ppmV)	$k^{H_3O^+}_{toluene}/k^{H_3O^+}_{butanone}$ [a]	$k^{NO^+}_{toluene}/k^{NO^+}_{butanone}$ [a]	$k^{O_2^+}_{toluene}/k^{O_2^+}_{butanone}$ [a]	Variation	$k_{toluene}/k_{butanone}$ of all ions [c]	k ($\times 10^{-11}$ cm^3/(molecule·sec)) [c]
293	1.9	1.8	11	1.58±0.10	1.45±0.06	1.46±0.08	8%	1.50±0.07	6.22±0.31
293	1.9	1.8	11	1.72±0.06	1.60±0.04	1.51±0.04	12%	1.61±0.10	
313	1.8	1.9	7.0	1.52±0.02	1.51±0.04	1.27±0.02	16%	1.43±0.14	5.63±0.55
Average k (± 2σ) over the temperature range 258-333 K									**5.85±0.15** [d]

The relative rate ratios determined for each pair of precursor ions (H_3O^+, NO^+ and O_2^+) for toluene ($k^{precursor\ ion}_{toluene}$) and the reference compound ($k^{precursor\ ion}_{reference}$) are given in the table as $k^{H_3O^+}_{toluene}/k^{H_3O^+}_{reference}$, $k^{NO^+}_{toluene}/k^{NO^+}_{reference}$, and $k^{O_2^+}_{toluene}/k^{O_2^+}_{reference}$. The reported relative rate ratio represents the averaged value of the ions' precursor ratio.

[a] Errors represent the 2σ fit precision and do not include systematic uncertainties

[b] Variation denotes the difference between the highest and the lowest relative rate ratios of the compound of interest and the reference, $k_{toluene}/k_{reference}$, values between the different precursor ions.

[c] Uncertainties quoted to the mean values are the 2σ standard deviations.

[d] Quoted uncertainty is the 2σ precision of the average value obtained from the linear fit of all measurements (see Fig. 7).

data from both IUPAC and NASA/JPL kinetics evaluation panels within 4%.

To conclude, in this section has been evidenced that THALAMOS is capable of measuring accurate gas-phase rate coefficients of atmospheric relevant reactions as a function of temperature. To the best of our knowledge, on European level, there is no other simulation chamber that has been used for gas phase kinetic studies in such a wide temperature range. Therefore, THALAMOS appears to be an innovative reference tool for temperature dependent investigation of atmospheric relevant processes extending and completing the capabilities of ASCs. Finally, we also present the kinetic and mechanistic investigation of Cl atoms initiated reaction with toluene, as a function of temperature.

2.2. *Cl atoms reaction rate coefficients with toluene*

In this section, temperature dependent Cl kinetics and reaction products with toluene, a common anthropogenic pollutant, are presented. Besides kinetics, product yields of benzaldehyde and benzyl alcohol - primary oxidation products - as a function of temperature were also determined, and a detailed mechanistic scheme is proposed.

2.2.1. *Rate coefficient measurements*

To the best of our knowledge, there are only room temperature kinetics studies for the reaction of Cl atoms with toluene in the literature (Atkinson and Aschmann, 1985; Fantechi et al., 1998; Markert and Pagsberg, 1993; Noziere et al., 1994; Shi and Bernhard, 1997; Wallington et al., 1988). In this work, the rate coefficients of the Cl reaction with toluene were determined between 253 and 333 K, at 1 atm (zero air) employing relative rate methods. Cl reaction with ethane, methanol, and butanone were used as references, and their temperature dependent rate coefficients were taken from IUPAC kinetic database (Atkinson et al., 2006), i.e., $k_{(ethane + Cl)} = 7.05 \times 10^{-11} \exp(-\frac{60}{T})$ cm^3/(molecule·sec) recommended over 180-330 K; $k_{(methanol + Cl)} = 7.10 \times 10^{-11} \exp(-\frac{75}{T})$ cm^3/(molecule·sec) recommended over 200-500 K; $k_{(butanone + Cl)} = 3.05 \times 10^{-11} \exp(\frac{80}{T})$ cm^3/(molecule·sec) recommended over 200-450 K, where $k_{(M + Cl)}$ is the rate coefficient of the Cl reaction with the compound M. Reactants loss and stable products formation were monitored via SIFT-MS. In particular, toluene, methanol and butanone, were monitored using all the three precursor ions of the MS, i.e. H_3O^+, NO^+ and O_2^+, and the characteristic mass intensities of each compound are given in Table 1. Consequently, the relative rate ratios were determined for each pair of precursor ions for toluene ($k^{precursor\ ion}_{toluene}$) and the reference compound ($k^{precursor\ ion}_{reference}$) i.e., $k^{H_3O^+}_{toluene}/k^{H_3O^+}_{reference}$, $k^{NO^+}_{toluene}/k^{NO^+}_{reference}$ and $k^{O_2^+}_{toluene}/k^{O_2^+}_{reference}$, respectively. The reported relative rate ratio represents the averaged value of the ions' precursor ratio. However, in the cases that ethane was used as reference

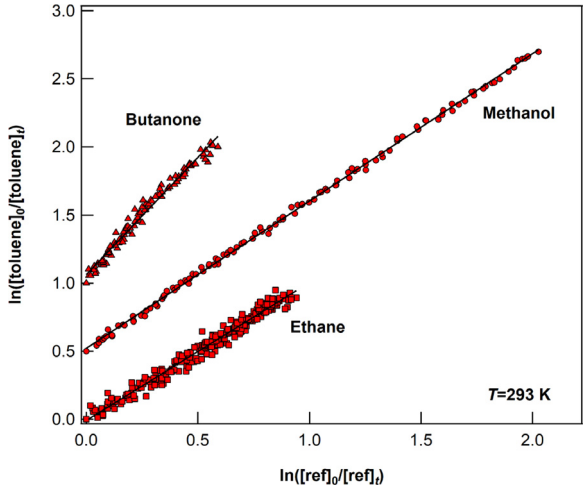

Fig. 6 – Example of relative rate plots for the Cl + toluene reaction obtained at 293 K using the reference compounds labeled on the graph. For the relative rate data displayed, the H_3O^+ precursor ion of the SIFT-MS was selected to monitor in real time the concentrations of toluene and the reference. For clarity the measurements have been displaced vertically by 0.5 for methanol and 1 for butanone. $[toluene]_0$, $[ref]_0$, $[toluene]_t$, $[ref]_t$ are the initial concentrations of the compound of interest and that of the reference, with no OH radicals present (light-sources off), at t = 0 and at discrete reaction times t, respectively.

($k_{ethane}^{precursor\ ion}$) and due to the low proton transfer affinity of the H_3O^+ and NO^+ (low detection sensitivity), only O_2^+ precursor ion was selected to monitor its concentration. Therefore, the relative rate ratios are given by the expressions $k_{toluene}^{H_3O^+}/k_{ethane}^{O_2^+}$, $k_{toluene}^{NO^+}/k_{ethane}^{O_2^+}$ and $k_{toluene}^{O_2^+}/k_{ethane}^{O_2^+}$, while the mean relative rate coefficients were obtained by averaging the values of the aforementioned fractions. Table 3 summarizes the conditions that experiments carried out, the relative rate ratios and the obtained rate coefficients at each temperature. Typical relative rate kinetic profiles at 293 K are presented in Fig. 6. The lines are linear least-squares fits of the data and the fit results are given in Table 3. It should be pinpointed that as shown in Fig. 6 a slight deviation from straight line fitting was observed, when butanone was used as reference compound. This trend is a model-example that demonstrates vulnerability of RR methods when compounds or references might be involved in secondary processes (e.g photolysis, on-surface or gas-phase hydrolysis, polymerization etc.). Therefore, although the measurements, in which butanone was used as reference, led to reasonable kinetic results, within the measurements uncertainties, the number of the experiments were limited.

The results from this study are comparatively given in Fig. 7, along with the existing literature data. It is evident that our room temperature values are in excellent agreement with the ones in the literature. Averaged rate coefficient at 295 ± 3 K was measured to be (5.82 ± 0.19) × 10^{-11} cm^3/(molecule·sec). In addition, no temperature dependence of the reaction rate coefficient was measured for the reaction of Cl atoms with toluene between 253 and 333 K, leading to a value (5.85 ± 0.12) × 10^{-11} cm^3/(molecule·sec). The latter suggests a complex reaction mechanism that proceeds via adduct formation. Although no temperature dependent experimental data exist in the literature Huang et al. (2012) have theoretically studied the reaction using ab-initio calculations reporting a strong positive temperature dependence of the rate coefficient in the range 298 – 1000 K. However, there are no data available at lower temperatures. The authors propose that the reaction mainly proceeds through -H atom abstraction from the methyl group of toluene (Huang et al., 2012).

2.2.2. Product study and proposed reaction mechanism

The mechanistic investigation and product analysis of the Cl atoms reaction with toluene was carried out in the temperature range 273 – 333 K using SIFT-MS as detection technique. Benzaldehyde and benzyl alcohol were identified as primary degradation products. Traces of benzyl hydroperoxide were also observed. The precursor ions and the mass spectral intensities used for the products detection with the MS are given in Table 1. All products were quantified using MS that was calibrated by (i) flowing a standard reference gas mixture, e.g., known concentration for each compound (toluene, benzaldehyde and benzyl alcohol) or (ii) by injecting known amount of the compounds (in the liquid or gas-phase as mixture diluted in air as discussed in section admission and mixing of compounds) inside THALAMOS and following their concentration with SIFT-MS. The second calibration method was applied in order to account for the impact of temperature on the calibration factor of the compounds. It should be noted that at sub-ambient temperatures, benzyl alcohol was not calibrated, since it was very lossy on the wall surfaces due to the low vapor pressure (<0.2 Torr at 293 K and ca. 1.6 Torr at 333 K). Therefore, the calibration factor determined at room temperature was used to estimate the corresponding product-yields. The estimated error to the concentration measurements was ~7% for toluene and benzaldehyde, and ~15% for benzyl alcohol due to its sticky nature. Benzyl hydroperoxide was not available and the MS calibration was not feasible. Therefore, the theoretical concentrations included in the instrument's software were used instead. In addition, separate photolysis tests for benzaldehyde and benzyl alcohol in the chamber were carried out leading to negligible photolysis rates (k_{phot} ~10^{-5} sec^{-1}) in the temperature range 273 – 333 K.

Typical temporal profiles for toluene consumption and benzaldehyde and benzyl alcohol formation are presented in Appendix A Fig. S4, at 333 K. It is worth to note that although benzaldehyde was rapidly produced, benzyl alcohol was appeared to be formed at delayed times when substantial toluene consumption observed. This delayed production of Benzyl alcohol suggests either that benzyl alcohol is a secondary reaction product and/or, less importantly, delayed mixing due to its low volatility. In order to further look into benzyl alcohol formation, separate measurements were carried out, in which the reaction mixture was irradiated for ~10 min and then lights were off until benzyl alcohol reach a steady-state. The above cycle was repeated several times, until toluene consumption due to its reaction with Cl atoms to be at least 50%.

Furthermore, to complement and cross validate the results obtained with the MS, an experiment was carried out at room temperature coupling the FTIR to the chamber. The concentrations of toluene and molecular chlorine used were rather high, in the range of 55 ppmV each. Benzaldehyde and benzyl alcohol were also identified by FTIR, along with HCl formation. The reference spectra of toluene and the formed organics were recorded in separate experiments after introducing a known concentration of each compound in the FTIR cell. Toluene and benzaldehyde concentrations were determined using the well-established cross section values at 739.8 and 1731 cm^{-1} for toluene and benzaldehyde, respectively. Although benzyl alcohol was observed FTIR detection sensitivity was not adequate to accurately measure its concentration. Toluene total loss was approximately 45%. Typical IR spectra recorded during the reaction, as well as reference spectra of toluene, benzaldehyde and benzyl alcohol are given in Appendix A Fig. S5.

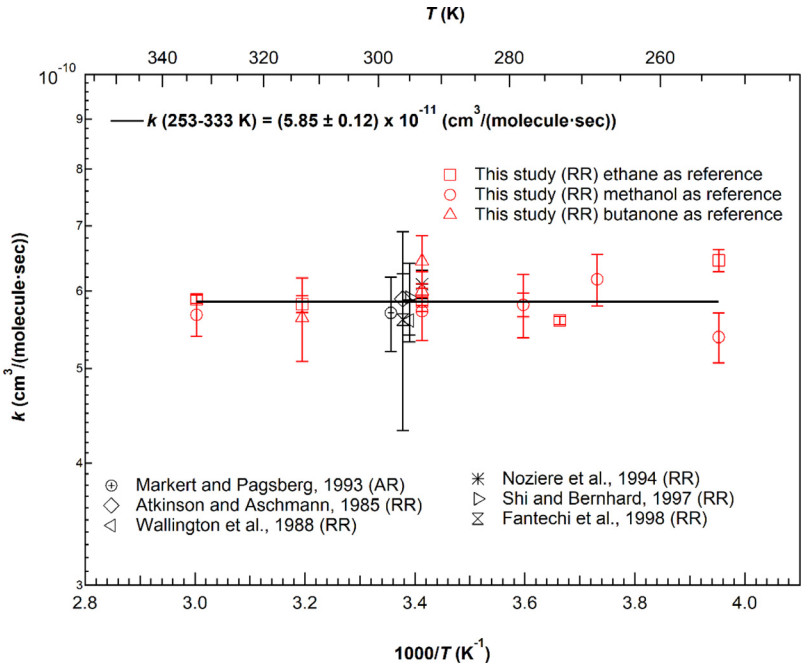

Fig. 7 – Temperature dependent data for the reaction of Cl atoms with toluene. The error bars quoted in our measurements correspond to the standard deviation of the mean values determined for the different precursor ions. The solid line corresponds to the average value of all measurements performed in the range of 253 to 353 K.

Table 4 summarizes the experimental conditions and the yields of the major products in the temperature range 273 – 333 K. The yield of the detected products (Y_{DP}) was determined as the ratio of the product concentration formed to the concentration of toluene consumed during the course of the reaction:

$$Y_{PD} = \Delta[\text{product}]/\Delta[\text{toluene}] \quad (4)$$

where Δ[product] correspond to the concentration of the product formed and Δ[toluene] the consumed concentration of toluene.

It should be noted that product yields determination was based on the initial data of the photo-oxidation experiment, where Cl atoms are principally consumed by toluene and side reactions of the products formed with Cl atoms are negligible compared to formation rate, within the experimental uncertainties. Benzaldehyde was found to be the major product formed. Typical plots displaying the consumption of toluene and the formation of benzaldehyde with the SIFT-MS and the FTIR are given in Fig. 8. The total yield of benzaldehyde was independent of temperature with an average value of 0.80 ± 0.05 (Fig. 8). The yield of benzyl alcohol was measured to be ~0.11 at 293 K (Appendix A Fig. S6). At 273 K the yield of benzyl alcohol was decreased by a factor of 2 compared to the room temperature value, but this might be an artifact of the system due to the high sticky efficiency and the significantly decreased vapor pressure of the compound at lower temperatures. Regarding benzyl hydroperoxide, an upper limit of 0.001 can be given based on the theoretical concentrations measured with SIFT-MS.

There is a large disagreement between literature studies regarding the absolute yield of the products formed from the Cl initiated oxidation of toluene. Nozière et al. (1994) conducted experiments in a 140 L Pyrex reactor using relatively high concentrations of toluene (6-33 ppmV) and Cl_2 (132 ppmV), and they observed benzaldehyde, as the major product, with a yield of 0.41 ± 0.04. The formation of benzyl alcohol, and benzyl hydroperoxide was also reported with yields 0.15 ± 0.03 and 0.18 ± 0.04, respectively (Noziere et al., 1994). On the contrary, Fantechi et al. (1998) did not detect either benzyl alcohol or benzyl hydroperoxide. According to these authors, the major end-oxidation product was benzaldehyde with a yield of 0.62 ± 0.30. Wang et al. (2005), recently, reported product-yields for benzaldehyde and benzyl alcohol of 0.84 ± 0.07 and 0.11 ± 0.02, respectively. The benzyl hydroperoxide formation was not included in Wang et al.'s analysis (Wang et al., 2005). However, under their experimental conditions, i. e., atmospheric pressure and 296 K, benzyl hydroperoxide concentration is expected to be very low, especially since the total products yield is almost unity (0.95 ± 0.08). The product yields measured in the current study at 293 K for benzaldehyde and benzyl alcohol are in excellent agreement with those of Wang et al. (2005). In addition, no temperature dependence of the yields was observed, although the upper limit for benzyl hydroperoxide (0.001) is significantly lower than the reported value by Nozière et al. (1994), it is in agreement with the observations from Fantechi et al. (1998) and Wang et al. (2005). Although Wang et al. (2005) suggested that dark reactions in Nozière et al.'s system (1994) might be responsible for the observed discrepancy, there are no clear evidence and the issue is currently unresolved (due to high initial concentrations of toluene and Cl_2 used).

Taking into account that the major products formed from the Cl initiated oxidation of toluene preserved the aromatic structure and that no chlorinated organic compounds were observed, it seems that reaction proceeds via direct or indirect -H atom abstraction and not by addition of Cl to the aromatic ring. The HCl formation observed in our FTIR experiment, as well as in other studies (Fantechi et al., 1998) provide with further indications that enhance the latter statement's validity. Further, a comparison between benzene ($k = 1.3 \times 10^{-15}$ cm^3/(molecule·sec) at 295 K (Shi and Bernhard, 1997) or $< 5.0 \times 10^{-16}$ (Noziere et al., 1994)) and toluene determined in this work ($k = 5.82 \times 10^{-11}$ cm^3/(molecule·sec) at 298 K) was conducted, and reactivity towards Cl atoms reveals that association mechanism is a highly unlikely reaction pathway and the replacement of one hydrogen with a methyl group

Table 4 – Summary of experimental conditions and product yields for the gas phase reaction of toluene with Cl atoms.

T (K)	$[Toluene]_0$ (ppmV)	$[Cl_2]_0$ (ppmV)	Benzaldehyde					Benzyl alcohol			
			Yield$^{H_3O^+}$ (%)[a]	Yield$^{NO^+}$ (%)[a]	Yield$^{O_2^+}$ (%)[a]	Average yield of all ions (%)	Yield FTIR (%)[a]	Yield$^{H_3O^+}$ (%)[a]	Yield$^{NO^+}$ (%)[a]	Yield$^{O_2^+}$ (%)[a]	Average yield of all ions (%)[b]
273	4.0	10.0	82±8	72±7	80±8	78±5	nd	5±1	4±1	6±1	5±1
293	4.0	10.0	88±9	90±9	84±8	87±3	nd	9±2	9±2	10±2	10±2
293	4.0	7.0	78±8	73±7	83±8	78±5		11±2	11±2	13±3	12±3
293	12.0	22.0	72±7	70±7	75±8	72±3		nd	nd	nd	nd
293	52.0	55.0	85±8	82±8	92±9	86±5	75±7	17±3	17±3	12±2	16±3
333	3.0	11.0	85±8	74±7	86±8	82±7	nd	13±3	11±2	14±3	13±2
333	3.0	9.0	90±9	85±8	82±8	86±4		10±2	12±2	14±3	12±2
Total yield (independent on T)						80±5[b]					11±4[b]

nd: not determined; Yield$^{H_3O^+}$, Yield$^{NO^+}$ and Yield$^{O_2^+}$: the yield of the products formed deploying selective ion flow tube mass spectrometry (SIFT-MS) for each of the precursor ions H_3O^+, NO^+ and O_2^+; Average yield of all ions: the average yield of each product formation using SIFT-MS; Yield FTIR: the yield of benzaldehyde demined deploying Fourier transformed infrared spectroscopy (FTIR).

[a] Errors represent the 2σ fit precision and includes the uncertainty to concentrations determination.

[b] Uncertainties quoted to the mean values are the standard deviation.

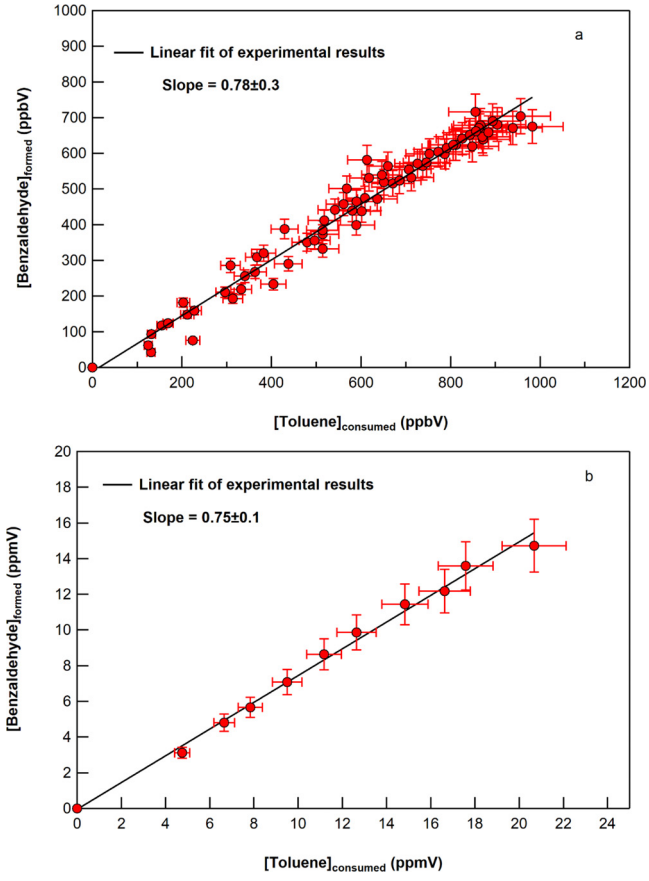

Fig. 8 – Typical concentration plots of benzaldehyde formed versus toluene consumed at 293 K with (a) the SIFT-MS using the H_3O^+ precursor ion to monitor the corresponding compounds and (b) the FTIR. Error bars reflects the uncertainty to the determination of compounds concentrations. The lines are the linear fit of experimental results (not forced to pass through the origin). The slope corresponds to the product yield of benzaldehyde (±2σ precision).

drastically increases toluene's reactivity, since -CH_3 hydrogen metathesis does not affect ring's aromaticity. However, it is worth to mention that in order to further investigate if the hydrogen metathesis proceeds via adduct formation in a stepwise process or via direct abstraction quantomechanical molecular calculations could be of use, although it was beyond the scope of the present study. Theoretical calculations performed by Huang et al. (2012) also support the experimental observations. In particular, it is proposed that the -H atom is mainly abstracted from the -CH_3 group of toluene, while the rest of the potent -H atom elimination sites, such as ortho, meta and para positions have a negligible contribution if any. The latter is also consistent with previously reported experimental studies (Fantechi et al., 1998; Markert and Pagsberg, 1993; Wang et al., 2005). Thus, in Fig. 9, a mechanistic scheme is proposed for the oxidation of toluene from Cl atoms.

Assuming that toluene is mainly removed from the atmosphere via the gas phase reactions with OH radicals and Cl atoms, and reactions with O_3 and NO_3 are expected to be negligible, the atmospheric lifetime (τ_x, where x is the corresponding oxidant) can be estimated using the expressions:

$$\tau_{OH} = \frac{1}{k_{OH} \times [OH]} \quad (5)$$

Table 5 – Toluene atmospheric lifetime include both OH and Cl initiated tropospheric oxidation.

Scenario 1			Scenario 2		
τ_{OH} (hours)	τ_{Cl} (hours)	τ_{eff} (hours)	τ_{OH} (hours)	τ_{Cl} (hours)	τ_{eff} (hours)
22.7	955	22.2	22.7	47.7	15.4

Two different scenarios with regard the globally averaged diurnal OH radicals and Cl atoms concentrations have been employed. OH levels remained stable in both cases [OH] 2×10^6 radical/cm^3, while the extremes of diurnally averaged Cl concentration levels were used to include both free troposphere (Scenario 1: [Cl] 5×10^3 atom/cm^3) and local characteristics of urban and/or coastal environment (Scenario 2: [Cl] 1×10^5 atom/cm^3).
τ_{OH} and τ_{Cl}: toluene atmospheric lifetime due to its degradation by OH radicals and Cl atoms respectively; τ_{eff}: the effective lifetime of toluene.

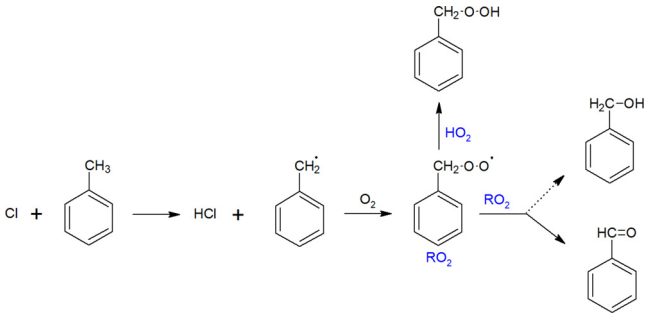

Fig. 9 – Proposed reaction mechanism for the oxidation of toluene from Cl atoms. The dash arrow is used to indicate the possible formation of a secondary product.

and

$$\tau_{Cl} = \frac{1}{k_{Cl} \times [Cl]} \quad (6)$$

where k_{OH} and k_{Cl} are the bimolecular rate coefficients for the corresponding reactions of toluene with OH radicals (i.e. 6.12×10^{-12} cm^3/(molecule·sec) at 300 K) and Cl atoms (i.e. 5.82×10^{-11} cm^3/(molecule·sec) at 295 ± 3 K average value of all studies) and [OH] and [Cl] are the diurnally averaged concentrations of OH radicals and Cl atoms in the environment of reference. Assuming an average tropospheric concentration of OH, i.e. 2×10^6 radical/cm^3 and an average boundary layer concentration of Cl, i.e. 10^4 atom/cm^3 respectively (Hein et al., 1997). OH radicals are expected to be the dominant sink, leading to an estimated lifetime of about one day (1 day). In urban and coastal areas though, where Cl atoms abundance is significant higher (Spicer et al., 1998), Cl chemistry will substantially reduce the globally averaged lifetime of toluene, even locally, in the troposphere (Table 5), which might be important for such short-lived compounds. On the contrary, in indoor environments where OH radical concentrations are significant lower, e.g., 10^4 to 10^5 molecule/cm^3 (Carslaw, 2007; Sarwar et al., 2002) and Cl levels substantially increased due to the use of Cl-containing cleaning products and other indoor materials, Cl atoms might be of equal importance with or dominate over OH radicals.

3. Conclusions

In the current study, we present a recently designed and developed photochemical chamber, THALAMOS, with a wide temperature range thermostatic ability, 233 – 373 K. THALAMOS is equipped with in-line FTIR, SIFT-MS and GC-MS complementary detection techniques that allow internal cross-validation of various type of quantitative measurements, such as kinetics and product-yields studies. A detailed description of the facility, the instrumentation and the characterization of the conditions has been realized. The first kinetic results employing relative rate methods obtained during THALAMOS validation are also presented. Applying the relative rate method, and studying the temperature dependence of two well documented reactions it was evident that THALAMOS is capable of producing highly precise and accurate temperature kinetic data for atmospheric relevant, i.e., OH and Cl reactions. Furthermore, the kinetics and the mechanism for the Cl reaction with toluene was studied within a wide temperature range. The kinetic measurements carried out in THALAMOS revealed that Cl-initiated degradation of toluene is important in coastal areas and/or indoor environments. Benzaldehyde and benzyl alcohol were identified as the major Cl initiated end-oxidation products and the yields were measured to be 0.80 ± 0.05 and 0.11 ± 0.04, respectively. The present results are in excellent agreement with the ones from Wang et al. (2005). THALAMOS is oriented to be a unique tool for temperature dependent studies in the gas or heterogeneous phases, targeted to elucidate the impact of temperature to secondary organic aerosol formation, as well as to simulate extreme temperatures and humidity conditions (i.e. $T > 25$°C, RH > 60%, typical for Southern countries). The latter aims to test the efficiency of depolluting materials and to assist in sensors calibrations under extreme indoor or outdoor conditions.

Declaration of competing interest

The authors declare that they have no known competing financial interests or personal relationships that could have appeared to influence the work reported in this paper.

Acknowledgments

This article is dedicated to the memory of Dr. Ian Barnes from the Institute for Atmospheric and Environmental Research, University of Wuppertal, Germany, one among the leaders of chemical kinetics who inspired many scientists of our generation. This work is part of the chemical and physical properties of the atmosphere (CaPPA) project funded by the Agence Nationale de la Recherhe (ANR) through the programme d'investissements d'avenir PIA (No. ANR-11-LABX-0005-01), the "Hauts-de-France" Regional Council and the European Regional Development Fund (ERDF). A. Tomas and M. Romanias are thankful to the Institut National des Sciences de L'univers (INSU) les Enveloppes Fluides et L'environnement-Chimie de L'atmosphère (LEFE-CHAT) program for financial support. N. Osseiran acknowledges support from Labex CaPPA for his graduate fellowship. V.C Papadimitriou acknowledges

support from Labex CaPPA for his short term visit at the institute mines telecom (IMT) Lille Douai. M. E. Angelaki acknowledges support from the project make our planet great again (MOPGA) for her short term visit at IMT Lille Douai, and the Greek sate scholarships foundation (IKY) program that funds her PhD.

Appendix A. Supplementary data

Supplementary material associated with this article can be found in the online version at doi:10.1016/j.jes.2020.03.036.

REFERENCES

Akimoto, H., Hoshino, M., Inoue, G., Sakamaki, F., Washida, N., Okuda, M., 1979. Design and characterization of the evacuable and bakable photochemical smog chamber. Environ. Sci. Technol. 13, 471–475.

Atkinson, R., Aschmann, S.M., 1985. Kinetics of the gas phase reaction of Cl atoms with a series of organics at 296 ± 2 K and atmospheric pressure. Int. J. Chem. Kinet. 17, 33–41.

Atkinson, R., Baulch, D.L., Cox, R.A., Crowley, J.N., Hampson, R.F., Hynes, R.G., et al., 2006. Evaluated kinetic and photochemical data for atmospheric chemistry: Volume II - gas phase reactions of organic species. Atmos. Chem. Phys. 6, 3625–4055.

Beichert, P., Wingen, L., Lee, J., Vogt, R., Ezell, M.J., Ragains, M., et al., 1995. Rate constants for the reactions of chlorine atoms with some simple alkanes at 298 K: Measurement of a self-consistent set using both absolute and relative rate methods. J. Phys. Chem. 99, 13156–13162.

Bryukov, M.G., Slagle, I.R., Knyazev, V.D., 2003. Kinetics of reactions of Cl atoms with ethane, chloroethane, and 1,1-dichloroethane. J. Phys. Chem. A 107, 6565–6573.

Burkholder, J.B., Sander, S.P., Abbatt, J., Barker, J.R., Huie, R.E., Kolb, C.E., et al., 2015. Chemical kinetics and photochemical data for use in atmospheric studies, Evaluation No. 18. JPL Publication 15-10. Jet Propulsion Laboratory, Pasadena.

Campbell, I.M., Mclaughlin, D.F., Handy, B.J., 1976. Rate constants for reactions of hydroxyl radicals with alcohol vapours at 292 K. Chem. Phys. Lett. 38, 362–364.

Can, E., Özden, Ü.Ö., Döğeroğlu, T., Gaga, E.O., 2015. Indoor air quality assessment in painting and printmaking department of a fine arts faculty building. Atmos. Pollut. Res. 6, 1035–1045.

Carslaw, N., 2007. A new detailed chemical model for indoor air pollution. Atmos. Environ. 41, 1164–1179.

Catoire, V., Lesclaux, R., Schneider, W.F., Wallington, T.J., 1996. Kinetics and mechanisms of the self-reactions of CCl_3O_2 and $CHCl_2O_2$ radicals and their reactions with HO_2. J. Phys. Chem. 100, 14356–14371.

Clyne, M.A.A., Walker, R.F., 1973. Absolute rate constants for elementary reactions in the chlorination of CH_4, CD_4, CH_3Cl, CH_2Cl_2, $CHCl_3$, $CDCl_3$ and $CBrCl_3$. J. Chem. Soc., Faraday Trans. 1 69, 1547–1567.

Davis, D.D., Braun, W., Bass, A.M., 1970. Reactions of $Cl_2P^{3/2}$: Absolute rate constants for reaction with H_2, CH_4, C_2H_6, CH_2Cl_2, C_2Cl_4, and c-C_6H_{12}. Int. J. Chem. Kinet. 2, 101–114.

Dillon, T.J., Hölscher, D., Sivakumaran, V., Horowitz, A., Crowley, J.N., 2005. Kinetics of the reactions of HO with methanol (210–351 K) and with ethanol (216–368 K). Phys. Chem. Chem. Phys. 7, 349–355.

Fantechi, G., Jensen, N.R., Saastad, O., Hjorth, J., Peeters, J., 1998. Reactions of Cl atoms with selected VOCs: Kinetics, products and mechanisms. J. Atmos. Chem. 31, 247–267.

Garzón, A., Moral, M., Notario, A., Ceacero-Vega, A.A., Fernández-Gómez, M., Albaladejo, J., 2010. Atmospheric reactions of (H)- and (D)-fluoroalcohols with chlorine atoms. Chem. Phys. Chem. 11, 442–451.

Greenhill, P.G., Ogrady, B.V., 1986. The rate-constant of the reaction of hydroxyl radicals with methanol, ethanol and (D_3)methanol. Aust. J. Chem. 39, 1775–1787.

Hazrati, S., Rostami, R., Fazlzadeh, M., Pourfarzi, F., 2016. Benzene, toluene, ethylbenzene and xylene concentrations in atmospheric ambient air of gasoline and CNG refueling stations. Air Qual. Atmos. Health 9, 403–409.

Hein, R., Crutzen, P.J., Heimann, M., 1997. An inverse modeling approach to investigate the global atmospheric methane cycle. Global Biogeochem. Cycles 11, 43–76.

Huang, M., Wang, Z., Hao, L., Zhang, W., 2012. DFT study on the abstraction and addition of Cl atom with toluene. Comput. Theor. Chem. 996, 44–50.

Jiménez, E., Gilles, M.K., Ravishankara, A.R., 2003. Kinetics of the reactions of the hydroxyl radical with CH_3OH and C_2H_5OH between 235 and 360 K. J. Photochem. Photobiol. A 157, 237–245.

King, M., 2016. The relative-rate technique for determining rate constants. ECG Environ. Briefs ECGEB No 13.

Kovács, G., Szász-Vadász, T., Papadimitriou, V.C., Dóbé, S., Bérces, T., Márta, F., 2005. Absolute rate constants for the reactions ofOHradicals withCH_3CH_2OH, CF_2HCH_2OH and CF_3CH_2OH. React. Kinet. Catal. Lett. 87, 129–138.

Leone, J.A., Flagan, R.C., Grosjean, D., Seinfeld, J.H., 1985. An outdoor smog chamber and modeling study of toluene-NOx photooxidation. Int. J. Chem. Kinet. 17, 177–216.

Lide, R.D., 2005. Physical Constants of Organic Compounds. CRC Handbook of Chemistry and Physics, 85th Ed. CRC Press.

Markert, F., Pagsberg, P., 1993. UV spectra and kinetics of radicals produced in the gas phase reactions of Cl, F and OH with toluene. Chem. Phys. Lett. 209, 445–454.

Morin, J., Romanias, M.N., Bedjanian, Y., 2015. Experimental study of the reactions of OH radicals with propane, n-pentane, and n-heptane over a wide temperature range. Int. J. Chem. Kinet. 47, 629–637.

United Nations, 2018. World urbanization prospects 2018: The speed of urbanization around the world.

Nelson, L., Rattigan, O., Neavyn, R., Sidebottom, H., Treacy, J., Nielsen, O.J., 1990. Absolute and relative rate constants for the reactions of hydroxyl radicals and chlorine atoms with a series of aliphatic alcohols and ethers at 298 K. Int. J. Chem. Kinet. 22, 1111–1126.

Niki, H., Maker, P.D., Savage, C.M., Breitenbach, L.P., 1980. An FTIR study of the Cl atom-initiated oxidation of CH_2Cl_2 and CH_3Cl. Int. J. Chem. Kinet. 12, 1001–1012.

Noziere, B., Lesclaux, R., Hurley, M.D., Dearth, M.A., Wallington, T.J., 1994. A kinetic and mechanistic study of the self-reaction and reaction with HO_2 of the benzylperoxy radical. J. Phys. Chem. 98, 2864–2873.

Oh, S., Andino, J.M., 2001. Kinetics of the gas-phase reactions of hydroxyl radicals with C1–C6 aliphatic alcohols in the presence of ammonium sulfate aerosols. Int. J. Chem. Kinet. 33, 422–430.

Orkin, V.L., Khamaganov, V.G., Martynova, L.E., Kurylo, M.J., 2011. High-accuracy measurements of OH· reaction rate constants and IR and UV absorption spectra: Ethanol and partially fluorinated ethyl alcohols. J. Phys. Chem. A 115, 8656–8668.

Orlando, J.J., 1999. Temperature dependence of the rate coefficients for the reaction of chlorine atoms with chloromethanes. Int. J. Chem. Kinet. 31, 515–524.

Overend, R., Paraskevopoulos, G., 1978. Rates of hydroxyl radical reactions. 4. Reactions with methanol, ethanol, 1-propanol, and 2-propanol at 296 K. J. Phys. Chem. 82, 1329–1333.

Papadimitriou, V.C., Prosmitis, A.V., Lazarou, Y.G., Papagiannakopoulos, P., 2003. Absolute reaction rates of chlorine atoms with CF_3CH_2OH, CHF_2CH_2OH, and CH_2FCH_2OH. J. Phys. Chem. A 107, 3733–3740.

Picquet, B., Heroux, S., Chebbi, A., Doussin, J.F., Durand-Jolibois, R., Monod, A., et al., 1998. Kinetics of the reactions of OH radicals with some oxygenated volatile organic compounds under simulated atmospheric conditions. Int. J. Chem. Kinet. 30, 839–847.

Ravishankara, A.R., Davis, D.D., 1978. Kinetic rate constants for the reaction of hydroxyl with methanol, ethanol, and tetrahydrofuran at 298 K. J. Phys. Chem. 82, 2852–2853.

Sarwar, G., Corsi, R., Kimura, Y., Allen, D., Weschler, C.J., 2002. Hydroxyl radicals in indoor environments. Atmos. Environ. 36, 3973–3988.

Sarzyński, D., Gola, A.A., Brudnik, K., Jodkowski, J.T., 2011. Kinetic study of the reaction of chlorine atoms with dichloromethane and D-dichloromethane in the gas phase. Chem. Phys. Lett. 514, 220–225.

Sellevåg, S.R., Nielsen, C.J., Søvde, O.A., Myhre, G., Sundet, J.K., Stordal, F., et al., 2004. Atmospheric gas-phase degradation and global warming potentials of 2-fluoroethanol, 2,2-difluoroethanol, and 2,2,2-trifluoroethanol. Atmos. Environ. 38, 6725–6735.

Shi, J., Bernhard, M.J., 1997. Kinetic studies of Cl-atom reactions with selected aromatic compounds using the photochemical reactor-FTIR spectroscopy technique. Int. J. Chem. Kinet. 29, 349–358.

Smith, D., Spanel, P., 2005. Selected ion flow tube mass spectrometry (SIFT-MS) for on-line trace gas analysis. Mass Spectrom. Rev. 24, 661–700.

Sørensen, M., Hurley, M.D., Wallington, T.J., Dibble, T.S., Nielsen, O.J., 2002. Do aerosols act as catalysts in the OH radical initiated atmospheric oxidation of volatile organic compounds? Atmos. Environ. 36, 5947–5952.

Spanel, P., Smith, D., 2013. Advances in on-line absolute trace gas analysis by SIFT-MS. Curr. Anal. Chem. 9, 524.

Tschuikow-Roux, E., Faraji, F., Paddison, S., Niedzielski, J., Miyokawa, K., 1988. Kinetics of photochlorination of mono- and disubstituted fluoro-, chloro-, and bromomethanes. J. Phys. Chem. 92, 1488–1495.

Wallington, T.J., Kurylo, M.J., 1987. The gas phase reactions of hydroxyl radicals with a series of aliphatic alcohols over the temperature range 240–440 K. Int. J. Chem. Kinet. 19, 1015–1023.

Wallington, T.J., Skewes, L.M., Siegl, W.O., 1988. Kinetics of the gas phase reaction of chlorine atoms with a series of alkenes, alkynes and aromatic species at 295 K. J. Photochem. Photobiol. A 45, 167–175.

Wang, L., Arey, J., Atkinson, R., 2005. Reactions of chlorine atoms with a series of aromatic hydrocarbons. Environ. Sci. Technol. 39, 5302–5310.

Wayne, P.H, Tully, F.P., 1988. Catalytic conversion of alcohols to alkenes by OH. Chem. Phys. Lett. 152, 183–189.

Wu, H., Mu, Y., Zhang, X., Jiang, G., 2003. Relative rate constants for the reactions of hydroxyl radicals and chlorine atoms with a series of aliphatic alcohols. Int. J. Chem. Kinet. 35, 81–87.